



The specific heat loss combined with the thermoelastic effect for an experimental analysis of the mean stress influence on axial fatigue of stainless steel plain specimens

G. Meneghetti, M. Ricotta, B. Atzori

University of Padova, Department of Industrial Engineering, via Venezia 1, 35131, Padova, Italy
giovanni.meneghetti@unipd.it, mauro.ricotta@unipd.it; bruno.atzori@unipd.it

ABSTRACT. The energy dissipated to the surroundings as heat in a unit volume of material per cycle, Q , was recently proposed by the authors as fatigue damage index and it was successfully applied to correlate fatigue data obtained by carrying out fully reversed stress- and strain-controlled fatigue tests on AISI 304L stainless steel plain and notched specimens. The use of the Q parameter to analyse the experimental results led to the definition of a scatter band having constant slope from the low- to the high-cycle fatigue regime. In this paper the energy approach is extended to analyse the influence of mean stress on the axial fatigue behaviour of un-notched cold drawn AISI 304L stainless steel bars. In view of this, stress controlled fatigue tests on plain specimens at different load ratios R ($R=-1$; $R=0.1$; $R=0.5$) were carried out. A new energy parameter is defined to account for the mean stress effect, which combines the specific heat loss Q and the relative temperature variation due to the thermoelastic effect corresponding to the achievement of the maximum stress level of the stress cycle. The new two-parameter approach was able to rationalise the mean stress effect observed experimentally. It is worth noting that the results found in the present contribution are meant to be specific for the material and testing condition investigated here.

KEYWORDS. Dissipated energy density; Mean stress effect; Fatigue; Thermoelastic temperature; Fatigue life estimation; Thermometric methods.

INTRODUCTION

The fatigue damage monitoring and the fatigue life assessment of materials and components can be experimentally performed by using the surface temperature. In fact for a given set of boundary conditions (i.e. load test frequency, room temperature, specimen geometry), the temperature of a material undergoing fatigue increases as the applied stress amplitude increases. Stoy Meyer [1] adopted the dissipated energy to evaluate the fatigue limit of plain steel specimens; in particular he measured the temperature increase of a steady stream of water covering the specimen. More recently, Curti et al. proposed the “limit temperature” [2] and later La Rosa and Risitano suggested an experimental procedure for the rapid determination of the material fatigue limit [3], based on the temperature measurement by using an infrared camera. Recently Risitano et al. proposed a fatigue life assessment method valid for variable amplitude fatigue [4] and a thermographic method to evaluate the material fatigue limit by means of a static tensile test [5]. Curà et al. developed a methodology for the rapid determination of the material fatigue limit, based on an iterative method to

recognise the temperature measurements obtained from specimens loaded by stress amplitude higher or lower than the fatigue limit [6]. Giancane et al. analysed the non-uniform temperature distribution in the case of aluminium alloys [7]. In ref. [8] an experimental procedure was proposed to evaluate the energy dissipated as heat in a unit volume of material per cycle, Q , starting from temperature measurements. The Q parameter was then adopted as a new experimental damage index useful for fatigue life estimations. Recently, the use of the Q parameter enabled us to rationalise several experimental results generated from constant amplitude, push-pull, stress- or strain-controlled fatigue tests on plain and notched hot rolled AISI 304 L stainless steel specimens [9, 10] as well as from cold drawn un-notched bars of the same steel under fully-reversed axial and torsional fatigue loadings [11]. Here we recall that notched specimens had either lateral U- or V- notches, with root radii equal to 3 or 5 mm, or a central hole with radius equal to 8 mm. Fig. 1 shows the axial and the torsional fatigue test results in terms of net-section stress amplitude σ_{an} or τ_a , respectively, the mean fatigue curves and the 10%-90% scatter bands. The figure reports also the inverse slope k of the curves, the stress-based scatter index $T_\sigma = \sigma_{a,10\%} / \sigma_{a,90\%}$ (T_τ) and the life-based scatter index $T_{N,\sigma}$ ($T_{N,\tau}$). In the case of strain-controlled fatigue tests, the stress amplitude reported in Fig. 1 is the value measured at half the fatigue life. Fig. 2 shows the same fatigue data re-analysed in terms of the Q parameter. In particular, the 10%-90% scatter band shown in the figure was fitted only on the fatigue data published in [10]. However, Fig. 2 shows that fatigue data obtained under axial and torsional fatigue tests [11] can be interpreted by the same scatter band. More than 120 fatigue data are included in the figure.

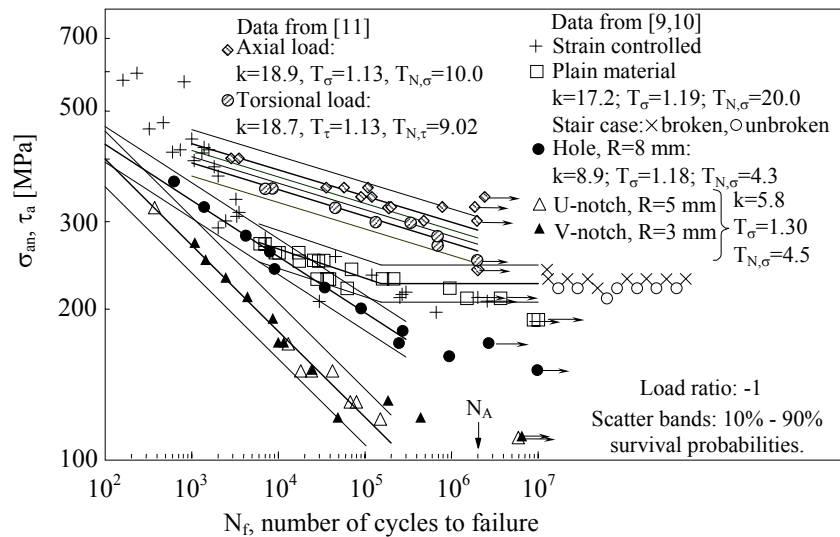


Figure 1: Fatigue data analysed in terms of net-section stress amplitude. Scatter bands are defined for 10% and 90% survival probabilities.

It is worth noting that the Q parameter is independent of the mechanical and thermal boundary conditions such as the specimen's geometry, load test frequency and room temperature [10]. By applying the energy balance equation, it was shown [8] that Q can be evaluated by stopping the fatigue test and then measuring the cooling gradient immediately after the test has been interrupted, according to Eq. (1):

$$Q \cdot f = -\rho \cdot c \cdot \frac{\partial T}{\partial t} \quad (1)$$

where

f is the load test frequency,

T is temperature,

t is time,

ρ is the material density

c is the material specific heat.

Concerning the stainless steel material analysed in the present paper, the material density ρ and the specific heat c were experimentally measured and resulted 7940 kg/m³ and 507 J/(kg K), respectively [12]. According to Eq. (1), it is possible to evaluate the thermal power ($Q \cdot f$) dissipated in steady state conditions by measuring the cooling gradient just after the



test interruption. Eq. (1) enables one to measure readily and in-situ the specific heat loss Q at any point of a specimen or a component undergoing fatigue loadings.

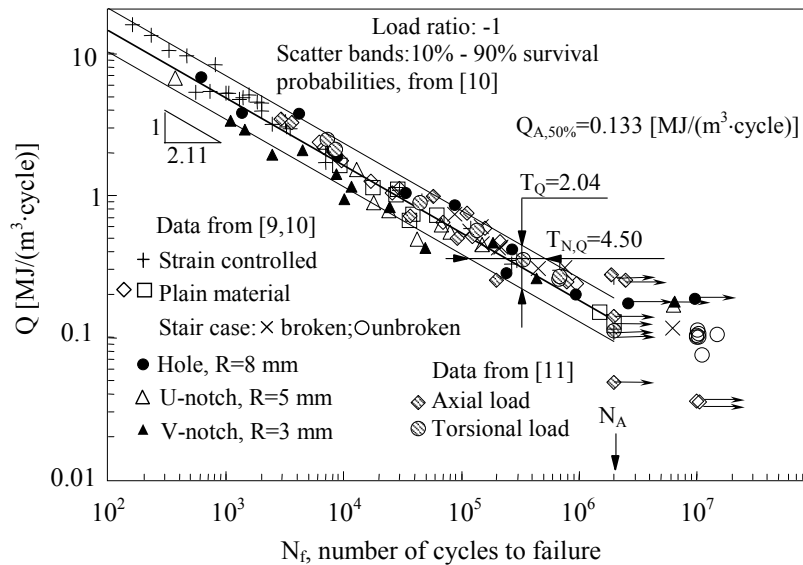


Figure 2: Fatigue data shown in Fig. 1 analysed in terms of energy released as heat by a unit volume of material per cycle. Scatter bands are defined for 10 and 90% survival probabilities.

Recently, the energy-based approach has been extended in order to take into account the presence of non-zero mean stresses [13]. In literature sound stress/strain-based approaches are available that include the influence of mean stresses; a common feature of them is to combine different mechanical parameters. Smith, Watson and Topper [14] proposed the SWT parameter to extend the Manson-Coffin approach:

$$SWT = \sqrt{\sigma_{\max} \cdot E \cdot \varepsilon_a} \quad (2)$$

where

ε_a is the applied strain amplitude,

E the material elastic modulus,

σ_{\max} the maximum stress.

Among the fracture mechanics-based approaches, Walker [15] and more recently Vasudevan et al. [16], Kujawsky [17, 18] and Stoychev and Kujawsky [19] proposed the parameter:

$$\Delta K_{eq} = \Delta K^{(1-\alpha)} \cdot K_{\max}^{\alpha} \quad (3)$$

to rationalise fatigue crack growth rate data, characterised by different values of the mean stress. In Eq. (3), ΔK and K_{\max} are the range and the maximum value of the stress intensity factor, respectively, and α is a best fitting parameter to determine from the experimental data.

Eq. (2) and (3) show that the driving force of the crack nucleation, Eq. (2), and propagation, Eq. (3), is characterised by two parameters: the amplitude (or range) of the driving force and its level (i.e. its maximum value). Both the parameters involved in Eq. (2) and Eq. (3) were interpreted by the authors of this paper in terms of energy, i.e. the hypothesis was formed that the fatigue strength depends on a thermodynamic exchange variable as well as on a state variable. After that, the Q parameter was identified as the exchange variable, whereas the thermoelastic temperature T_{the} was assumed as the state variable. The thermoelastic temperature T_{the} is the temperature that would be achieved by the material when loaded at the maximum stress level of the fatigue cycle, σ_{\max} , in an adiabatic process. T_{the} can be evaluated analytically or experimentally by loading the material in its elastic field and then by extending the temperature-applied stress relation up to the σ_{\max} value. The applied stress rate must be properly set in order to reduce the heat transfer between material and the surroundings, i.e. to make the loading process adiabatic. As it will be discussed in a dedicated section, it was found that such nearly adiabatic conditions can be reached in standard laboratory tests, at least for the material analysed in this paper.

Alternatively, the thermoelastic temperature T_{the} can be easily calculated from Eq. 4, which relates T_{the} to the maximum applied stress [20]:

$$\frac{T_{the}}{T_0} = -\left(\frac{\alpha}{\rho \cdot c}\right) \cdot \sigma_{max} = -K_m \cdot \sigma_{max} \quad (4)$$

where T_0 is the material temperature when the applied stress is equal to zero and α the material thermal expansion coefficient. Therefore the new equation proposed in the present paper to rationalise the mean stress influence on axial fatigue of stainless steel plain specimens is:

$$\left(\bar{Q} \cdot \left(\frac{|T_{the}|}{T_0}\right)^b\right)^m \cdot N_f = (\bar{Q})^m \cdot N_f = \text{const} \quad (5)$$

where b and m are material constants to evaluate by fitting the experimental data.

MATERIAL, SPECIMENS' GEOMETRY AND TEST PROCEDURE

The material selected for the experimental tests consisted of 25-mm-diameter AISI 304 L cold drawn bars, having a engineering tensile strength, R_m , and an engineering proof stress, $R_{p0.2}$, equal to 691 MPa and 468 MPa, respectively. The material adopted in this work is different from that analysed in [10], characterised by $R_m=700$ MPa and $R_{p0.2} = 315$ MPa. As to the material analysed in the present paper, the mechanical properties, the chemical composition, the Vickers hardness and the average grain size are listed in Tab. 1 [11].

E [MPa]	$R_{p0.2}$ [MPa]	R_m [MPa]	A [%]	HV ₃₀	C [%]	Si [%]	Mn [%]	Cr [%]	Mo [%]	Ni [%]	Cu [%]	Average grain size* [μm]
192200	468	691	43	199	0.013	0.58	1.81	18.00	0.44	8.00	0.55	35

Table 1: AISI 304 L material properties (*According to ASTM E 112 [21]).

Constant amplitude, stress-controlled fatigue tests were carried out on a servo-hydraulic MFL machines equipped with a 250 kN load cell and a MTS Testar II digital controller. Three different load ratios R ($R=-1$, $R=0.1$ and $R=0.5$) were adopted. In the case of load ratio equal to $R=-1$ and $R=0.1$, the specimens' geometry is shown in Fig. 3a, whereas that adopted for $R=0.5$ is reported in Fig. 3b. The load test frequency was selected in the range 1-30 Hz and as high as possible in order to maintain the stabilised temperature of the material below 70°C during the whole fatigue test. Then the fatigue test was suddenly stopped to measure the cooling gradient and to evaluate the Q parameter, according to the experimental procedure proposed in [8]. The fatigue tests were run until the specimen's failure or to 2 million cycles (run-out specimen).

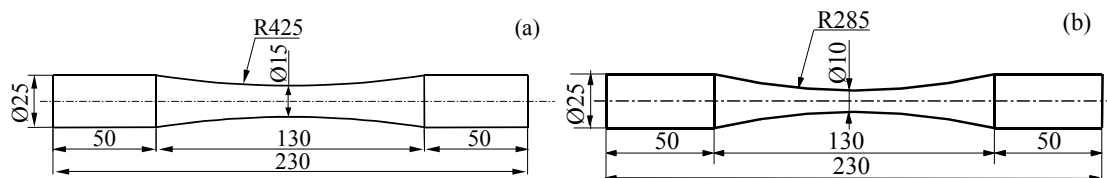


Figure 3: Specimens' geometry adopted for fatigue tests having a) load ratio $R=-1$ e $R=0.1$ and b) $R=0.5$.

To evaluate the thermoelastic material constant K_m , Eq. (4), load controlled ramps were executed at different load rates by means of a servo-hydraulic Schenck Hydropuls PSA 100 machine equipped with a 100 kN load cell and a Trio Sistemi RT3 digital controller.

During all tests, the specimen's temperature was measured by using a copper-constantan thermocouple having diameter of 0.127 mm, which was fixed at the specimen's centre by means of a silver-loaded conductive epoxy glue. Temperature



signals generated by the thermocouples were acquired by means of a data logger Agilent Technologies HP 34970A operating at a maximum sample frequency, f_{acq} , of 22 Hz (accuracy equal to 0.02 °C).

FATIGUE TEST RESULTS

Fig. 4 shows the fatigue test results and reports the mean curves in terms of the engineering stress amplitude σ_a , the 10%-90% survival probability scatter bands, the inverse slope k , the reference fatigue strength $\sigma_{A,50\%}$ evaluated at $N_A = 2$ million cycles with a survival probability equal to 50%, and the stress- as well as the life-based scatter index T_σ and T_N , respectively. The experimental data were statistically re-analyzed under the hypothesis of log-normal distribution of the number of cycles to failure with a 95% confidence level. It can be seen that the fatigue behaviour of the analysed material is significantly affected by the load ratio: in fact $\sigma_{A,50\%}$ evaluated under push-pull fatigue test ($R=-1$) is reduced of a factor equal to 1.27 and 1.86, in the case of $R=0.1$ and $R=0.5$, respectively.

It is worth noting that in all fatigue tests carried out by imposing a load ratio equal to $R=0.5$ and in many tests conducted at $R=0.1$, the maximum stress was higher than the material proof stress. Therefore, the cyclic material stabilisation was monitored by considering the axial displacement measured by the displacement transducer of the test machine. After stabilisation, the reduction of the specimen diameter ranged from 4.5% to 19.5% with respect to the initial diameter, depending on the applied stress amplitude.

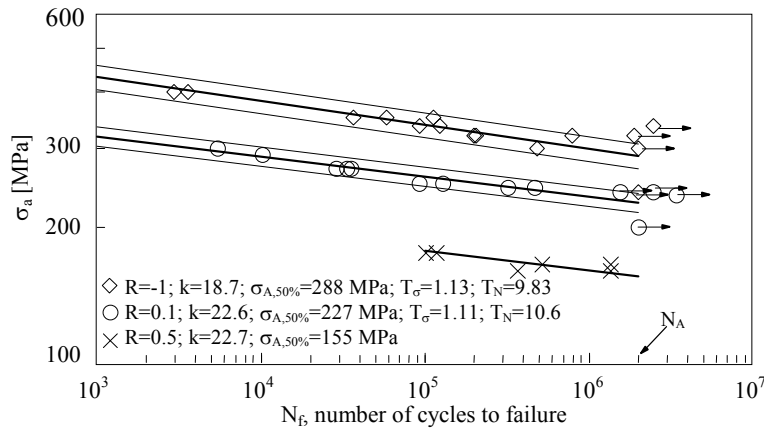


Figure 4: Fatigue data analysed in terms of engineering stress amplitude for different load ratios. Scatter bands are defined for 10% and 90% survival probabilities.

ENERGY-BASED FATIGUE TEST RESULTS

In order to evaluate the evolution of Q parameter, each fatigue test was interrupted several times. Fig. 5 shows some characteristic examples of Q values plotted against the number of cycles normalised with respect to the number of cycles to failure or, in the case of run-out specimens, with respect to 2 millions. One can observe that the Q values span in a range between 0.01 and 5 MJ/(m³·cycle) by considering the different load ratio analysed in this paper, in spite of a variation of σ_a from 155 to 400 MPa. According to [8], the fatigue test results were re-analyzed in terms of the characteristic value of Q measured at 50% of the number of cycles to failure or, in the case of run-out specimens, at 1 million cycles. Fig. 6 shows the results of the statistical analysis in the hypothesis of log-normal distribution of the number of cycles to failure N_f and constant scatter with respect to the energy dissipation level. The mean and the 10% - 90% survival probability curves fitting the experimental results with a confidence level of 95% have the following expression:

$$Q^k \cdot N_f = cost \tag{6}$$

The figure reports the inverse slope k of the curves, the mean energy value $Q_{A,50\%}$ at the reference fatigue life N_A of two million cycles and the energy- as well as the life-based scatter index T_Q and $T_{N,Q}$, respectively. Fig. 6 shows that the data

obtained by carrying out fatigue tests at different load ratios cannot be rationalised in a single scatter band by using the Q parameter.

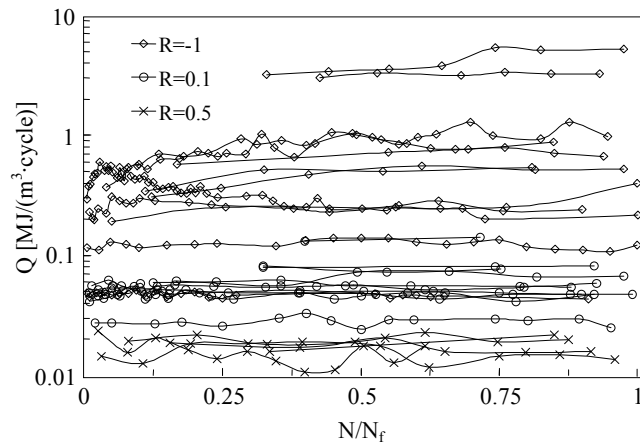


Figure 5: Measured Q trends against the number of cycles normalised with respect to the number of cycles to failure, N_f .

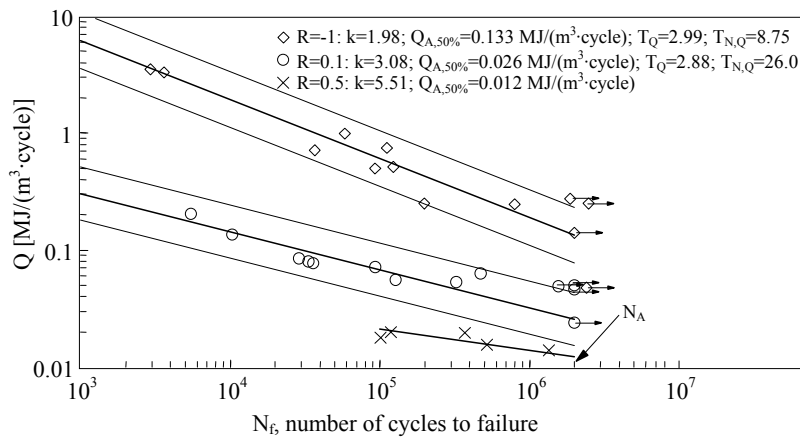


Figure 6: Fatigue data analysed in terms of energy released as heat by a unit volume of material per cycle. Scatter bands are defined for 10 and 90% survival probabilities.

EXPERIMENTAL EVALUATION OF THE THERMOELASTIC CONSTANT

To experimentally evaluate the thermoelastic constant K_m (see Eq. 4), load-controlled ramps at different load rates were carried out, aiming at the evaluation of the minimum stress-rate $\dot{\sigma}$ required to achieve adiabatic test conditions. Five stress rates were applied, namely $\dot{\sigma} = 5, 19, 37, 54$ and 73 MPa/s. The tests were conducted by applying an initial compressive stress equal to -150 MPa, followed by a ramp up to 150 MPa. The value of 150 MPa was chosen to guarantee the linear elastic behaviour of the analysed material. The adopted procedure can be summarised as follows:

- application of a compressive stress equal to -150 MPa applied to the specimen;
- holding of the compressive stress to allow for material thermal equilibrium with the surroundings (reference temperature T_0);
- execution of a tensile ramp up to 150 MPa with given $\dot{\sigma}$ value and measurement of the corresponding temperature drop. Since T_0 is the reference temperature at a stress of -150 MPa, the thermoelastic temperature T_{the} reached at the end of the test will be referred to a stress of 300 MPa.

Fig. 7 shows as an example the results of a test conducted at $\dot{\sigma} = 54$ MPa/s. Within the time window (t_f-t_i) , it can be observed that the temperature decreases from the initial value $T_0=301.25$ K. The stress range adopted to evaluate K_m corresponds to the stress variation in the time window $\Delta t=t_f-t_i$, ($\Delta\sigma=\sigma(t_f)-\sigma(t_i)$), that is 297 MPa in Fig. 7.

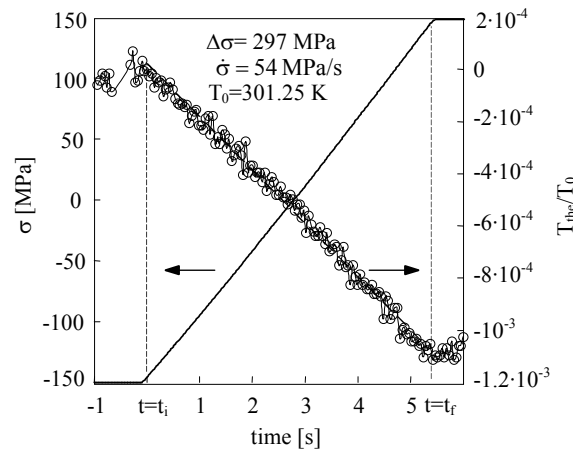


Figure 7: Example of static test and measured thermoelastic temperature variation.

The K_m values measured in all static tests are collected in Fig. 8. It can be observed that by increasing the applied stress rate, the scatter of the K_m values decreases and that a 5.4% variation of the K_m mean value was noticed (from $3.86 \cdot 10^{-12}$ to $3.65 \cdot 10^{-12} \text{ Pa}^{-1}$), by increasing the stress rate of a factor about 2 (from 37 to 73 MPa/s). Therefore from an engineering point of view, it can be concluded that adiabatic conditions can be reached by imposing a stress rate higher than 37 MPa/s, at least for the material and test conditions analysed in this paper. The final K_m value adopted was equal to $3.75 \cdot 10^{-12} \text{ Pa}^{-1}$, being the mean value measured for $\dot{\sigma}=37, 54$ e 73 MPa/s ; it is in good agreement with the theoretical value of $3.97 \cdot 10^{-12} \text{ Pa}^{-1}$ that can be calculated by using Eq. (4) and assuming $\alpha=16 \cdot 10^{-6} \text{ K}^{-1}$.

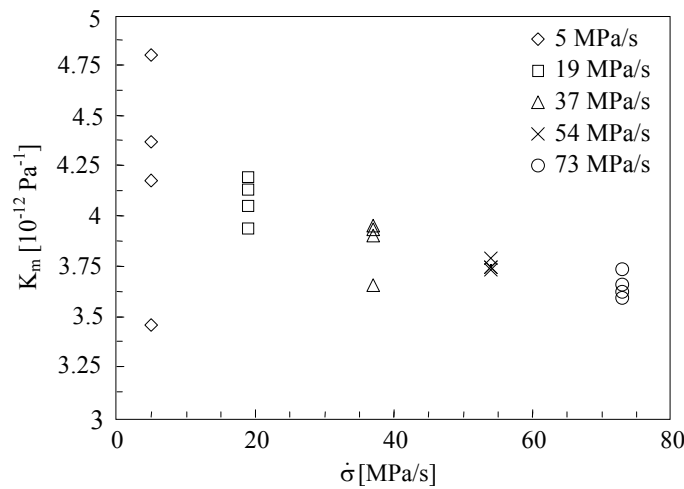


Figure 8: Experimental evaluation of the thermoelastic constant K_m of the analysed material.

THE NEW TWO-PARAMETER, ENERGY-BASED APPROACH APPLIED TO THE EXPERIMENTAL RESULTS

After evaluating the thermoelastic constant K_m , the thermoelastic temperature relevant to each specimen was calculated according to Eq. (4). Having in hands Q , $\left| \frac{T_{the}}{T_0} \right|$ and the number of cycles to failure N_f for each coupon, the parameters b and m of Eq. (5) were calculated. In more detail, the experimental results were plotted in a Q - $\left| \frac{T_{the}}{T_0} \right|$ plane, for a given number of cycles to failure, as shown in Fig. 9. By considering the available number of data and independently of the load ratio R , the fatigue results were divided in 4 groups, characterized by a different range of the number of cycles to failure ($N_f \leq 10000$ cycles; $20000 \leq N_f \leq 60000$ cycles; $80000 \leq N_f \leq 120000$ cycles e $300000 \leq N_f \leq 800000$ cycles).

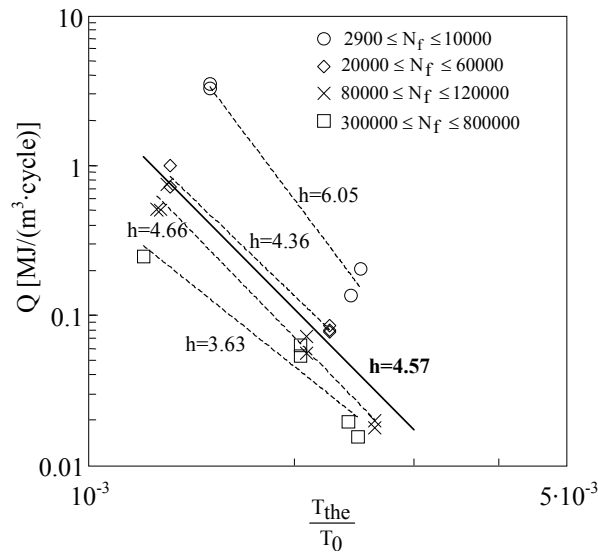


Figure 9: Evaluation of the b constant, Eq. (5).

Dashed regression lines in Fig. 9 (a log-log diagram) were calculated for each group. By considering the reduced variation among the b values from an engineering point of view, a unique b value was calculated and resulted equal to 4.57 (continuous line in Fig. 9).

After that, all available data were plotted in a \bar{Q} - N_f plane (see Eq. 5, $h=4.57$) and re-analyzed as a single population, independently of the load ratio, under the hypothesis of log-normal distribution of the number of cycles to failure and with a 95% confidence level. The result is shown in Fig. 10, where the mean line, the 10% - 90% survival probability curves, the inverse slope m , the equivalent energy $T_{\bar{Q}}$ and the life-scatter T_N indexes are plotted.

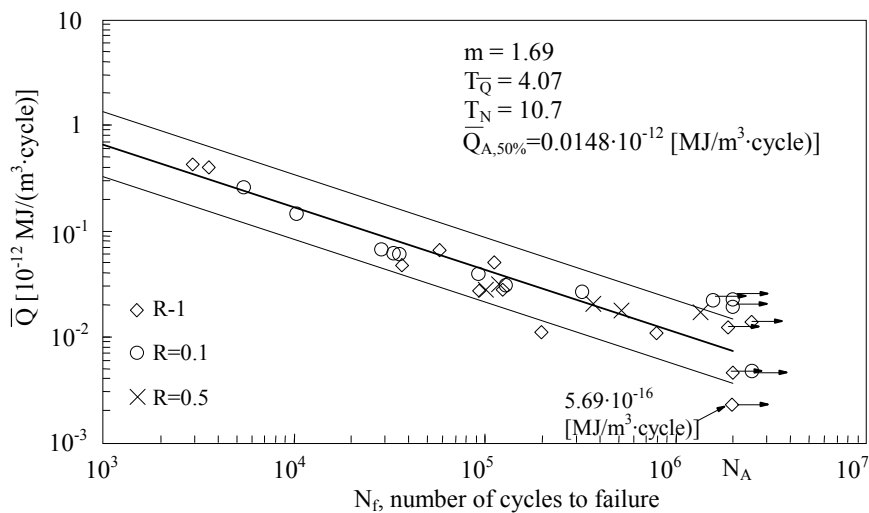


Figure 10: Fatigue data of Fig. 4 analysed in terms of the equivalent energy released as heat by a unit volume of material per cycle \bar{Q} . Scatter bands are defined for 10 and 90% survival probabilities.

By considering the stress amplitude as well as the dissipated energy-based curves (plotted in Fig. 4 and Fig. 6, respectively), one can appreciate that the new \bar{Q} parameter collapses all the fatigue data into a single scatter band having a constant slope from 10^3 to $2 \cdot 10^6$ cycles, despite the different load ratios involved. Moreover, it is worth noting that the scatter index T_N in Fig. 10 is very close to that relevant to the “ $R=-1$ ” and “ $R=0.1$ ” series presented in terms of stress amplitude (see Fig. 4) as well as to the “ $R=-1$ ” series expressed in terms of Q parameter (see Fig. 6).



CONCLUSIONS

In this paper a two parameter, energy-based approach has been presented to rationalise the influence of the load ratio on the fatigue behaviour of AISI 304 L cold drawn steel bars. Three different load ratios (namely $R=-1$, $R=0.1$ and $R=0.5$) were applied in the constant amplitude fatigue tests. The mean stress influence was considered by combining the specific heat loss with the thermoelastic temperature relevant to the maximum stress of the load cycle. The new two-parameter, energy-based method enabled us to collapse all fatigue test results in a single scatter band having a constant slope from 10^3 to $2 \cdot 10^6$ cycles. The scatter index resulted equal to that of single test series expressed in terms of stress amplitude. Static tests at different stress rate were carried out to experimentally measure the thermoelastic constant of the material, which is needed to calculate the thermoelastic temperature. It was observed that adiabatic test conditions required to measure the thermoelastic constant can be achieved by using a standard laboratory environment. This new approach has not been tested yet against materials different from that analysed in the present paper.

ACKNOWLEDGEMENTS

This work was carried out as a part of the Italian Research Program PRIN 2009Z55NWC of the Ministry of University and Scientific Research. The Authors would like to express their gratitude for financial support.

REFERENCES

- [1] Stoy Meyer, C.E., The determination of fatigue limits under alternating stress conditions, Proceedings of the Royal Society of London. Series A, 90 (1914) 411-425.
- [2] Curti, G., Geraci, AL., Risitano, A., A new method for rapid determination of the fatigue limit, *Ingegneria Automotoristica*, 42 (1989) 634-636. in italian.
- [3] La Rosa, G., Risitano, A., Thermographic methodology for rapid determination of the fatigue limit of materials and mechanical components, *Int J Fatigue*, 22 (2000) 65-73.
- [4] Risitano, A., Risitano, G., Cumulative damage evaluation of steel using infrared thermography, *Theor Appl Fract Mec*, 54 (2010) 82-90.
- [5] Risitano, A., Risitano, G., Determining fatigue limits with thermal analysis of static traction tests, *Fatigue Fract Eng Mater Struct*, 36 (2013) 631-639.
- [6] Curà, F., Curti, G., Sesana, R., A new iteration method for the thermographic determination of fatigue limit in steels *Int J Fatigue*, 27(4) (2005) 453-459.
- [7] Giancane, S., Chrysochoos, A., Dattoma, V., Wattrisse, B., Deformation and dissipated energies for high cycle fatigue of 2024-T3 aluminium alloy, *Theor Appl Fract Mec*, 52 (2009) 117-121.
- [8] Meneghetti G., Analysis of the fatigue strength of a stainless steel based on the energy dissipation, *Int J Fatigue*, 29 (2007) 81-94.
- [9] Meneghetti, G., Ricotta, M., The use of the specific heat loss to analyse the low- and high-cycle fatigue behaviour of plain and notched specimens made of a stainless steel, *Eng Fract Mec*, 81 (2012) 2-17.
- [10] Meneghetti, G., Ricotta, M., Atzori, B., A synthesis of the push-pull fatigue behaviour of plain and notched stainless steel specimens by using the specific heat loss, *Fatigue Fract Eng Mater Struct*, 36 (2013) 1306-1322.
- [11] Meneghetti, G., Ricotta, M., Negrisolò, L., Atzori, B., A synthesis of the fatigue behavior of stainless steel bars under fully reversed axial or torsion loading by using the specific heat loss, *Key Engineering Materials*, 577-578 (2014) 453-456.
- [12] Atzori, B., Meneghetti, G., Ricotta, M., Analysis of the fatigue strength under two load levels of a stainless steel based on energy dissipation. In: Proceedings of 14th International Conference on Experimental Mechanics ICEM14, Poitiers, France, (2010).
- [13] Meneghetti, G., Ricotta, M., Negrisolò, L., Sottana, G., Atzori, B., Sintesi del comportamento a fatica di un acciaio inossidabile AISI 304L a diversi rapporti di ciclo mediante l'uso combinato dell'energia dissipata e dell'effetto termoelastico, In: Proceedings of the 42° AIAS National Conference, Salerno (Italy), (2013).
- [14] Smith, KN., Watson, P., Topper, TH., A stress-strain function for the fatigue of metals, *J Mater*, 5 (1970) 767-778.



- [15] Walker, K., The effect of stress ratio during crack propagation and fatigue for 2024-T3 and 7075-T6 aluminum, ASTM STP, 462 (1970) 1-14.
- [16] Vasudevan, A.K., Sadananda, K., Glinka, G., Critical parameters for fatigue damage, Int. J. Fatigue, 23S (2001) S39-S53.
- [17] Kujawski, D., A new $(\Delta K^+ \cdot K_{\max})^{0.5}$ driving force parameter for crack growth in aluminum alloys, Int J Fatigue, 23 (2001) 733-740.
- [18] Kujawski, D., A fatigue crack driving force parameter with load ratio effects, Int. J. Fatigue, 23 (2001) S239-S246
- [19] Stoychev, S., Kujawski, D., Analysis of crack propagation using ΔK and K_{\max} , Int. J. Fatigue, 27 (2005) 1425-1431.
- [20] Audenino, A. L., Goglio, L., Rossetto, M., Metodi sperimentali per la progettazione, Levrotto&Bella, Torino, Italy (1997).
- [21] ASTM E112 - 12 Standard Test Methods for Determining Average Grain Size.